Printable thermo-optic polymer switches utilizing imprinting and ink-jet printing

Xiaohui Lin,[1,4] Tao Ling,[2,4] Harish Subbaraman,[3] L. Jay Guo,[2] and Ray T. Chen[1,*]

[1]*Department of Electrical and Computer Engineering, The University of Texas at Austin, 10100 Burnet Rd, Austin, TX 78758, USA*

[2] *Department of Electrical Engineering and Computer Science, University of Michigan, Ann Arbor, Michigan 48109*

[3] *Omega Optics, Inc, 10306 Sausalito Dr, Austin, TX 78759, USA*

[4]*These authors contributed equally.*

[*]*raychen@uts.cc.utexas.edu*

Abstract: We demonstrate a printable Thermo-Optic (TO) switch utilizing imprinting and ink-jet printing techniques. The material system, optical and thermal designs are discussed. Imprinting technique is used to transfer a 2 × 2 switch pattern from a flexible mold into a UV15LV polymer bottom cladding. Ink-jet printing is further used to deposit a SU-8 polymer core layer on top. Operation of the switch is experimentally demonstrated up to a frequency of 1 kHz, with switching time less than 0.5ms. The printing technique demonstrates great potential for high throughput, roll-to-roll fabrication of low cost photonic devices.

OCIS codes: (130.4815) Optical switching devices; (250.6715) Switching.

References and links

1. W. H. Wong, K. K. Liu, K. S. Chan, and E. Y. B. Pun, "Polymer devices for photonic applications," J. Cryst. Growth **288**(1), 100–104 (2006).
2. M. B. Christiansen, M. Schøler, and A. Kristensen, "Integration of active and passive polymer optics," Opt. Express **15**(7), 3931–3939 (2007).
3. X. H. Lin, X. Y. Dou, A. X. Wang, and R. T. Chen, "Polymer optical waveguide based bi-directional optical bus architecture for high speed optical backplane," Proc. SPIE **8267**, 826709 (2012).
4. H. Yu, X. Q. Jiang, J. Y. Yang, X. H. Li, M. H. Wang, and Y. B. Li, "The design of 2x2 polymer TIR switch based on thermal field analysis employing thermo-optic effect," Passive Components and Fiber-Based Devices **5623**, 174–183 (2005).
5. X. L. Wang, B. Howley, M. Y. Chen, and R. T. Chen, "4 x 4 nonblocking polymeric thermo-optic switch matrix using the total internal reflection effect," IEEE J Sel Top Quant **12**(5), 997–1000 (2006).
6. B. S. Lee, C. Y. Lin, A. X. Wang, and R. T. Chen, "Demonstration of a linearized traveling wave Y-fed directional coupler modulator based on electro-optic polymer," J. Lightwave Technol. **29**(13), 1931–1936 (2011).
7. D. H. Park, Y. Z. Leng, J. D. Luo, A. K. Y. Jen, and W. N. Herman, "High speed electro-optic polymer phase modulator using an in-plane slotline RF waveguide," Rf and Millimeter-Wave Photonics **7936** (2011).
8. W. H. Steier, A. Szep, Y. H. Kuo, P. Rabiei, S. W. Ahn, M. C. Oh, H. Zhang, C. Zhang, H. Erlig, B. Tsap, H. R. Fetterman, D. H. Chang, and L. R. Dalton, "High speed polymer electro-optic modulators," Leos 2001: 14th Annual Meeting of the IEEE Lasers & Electro-Optics Society, Vols 1 and 2, Proceedings, 188–189 (2001).
9. J. Y. Yang, Q. J. Zhou, and R. T. Chen, "Polyimide-waveguide-based thermal optical switch using total-internal-reflection effect," Appl. Phys. Lett. **81**(16), 2947–2949 (2002).
10. L. J. Guo, "Nanoimprint lithography: Methods and material requirements," Adv. Mater. (Deerfield Beach Fla.) **19**(4), 495–513 (2007).
11. S. H. Ahn and L. J. Guo, "High-speed roll-to-roll nanoimprint lithography on flexible plastic substrates," Adv Mater **20**, 2044–2049 (2008).
12. J. H. Min, H. Kim, B. Kim, and S. Kang, "Design of microlens array on aperture stop array to generate multi optical probes with spatial light modulation," Jpn. J. Appl. Phys. **47**(8), 6800–6803 (2008).
13. K. L. Lai, S. F. Hsiao, M. H. Hon, and I. C. Leu, "Patterning of polystyrene thin films by solvent-assisted imprint lithography and controlled dewetting," Microelectron. Eng. **94**, 33–37 (2012).
14. Y. L. Gao, J. Lin, P. Jin, J. B. Tan, G. Davies, and P. D. Prewett, "Stop grating for perfect replication of micro Fresnel lens by thermal imprinting," J. Micromech. Microeng. **22**(6), 065018 (2012).
15. S. W. Ahn, K. D. Lee, D. H. Kim, and S. S. Lee, "Polymeric wavelength filter based on a Bragg grating using nanoimprint technique," IEEE Photonic Tech L **17**(10), 2122–2124 (2005).
16. Y. J. Weng, Y. C. Weng, Y. C. Wong, S. Y. Yang, and H. K. Liu, "Fabrication of optical waveguide devices using electromagnetic assisted nanoimprinting," Proceedings of the 2009 International Conference on Signal Processing Systems, 910–912 (2009).

#179234 - $15.00 USD Received 8 Nov 2012; accepted 26 Dec 2012; published 18 Jan 2013

17. X. L. Wang, X. Y. Dou, X. H. Lin, and R. T. Chen, "Flexible polymer optical layer for board-level optical interconnects by highly durable metal imprinting method," Proc. SPIE **7607**, 76070R, 76070R-7 (2010).
18. M. Wang, J. Hiltunen, S. Uusitalo, J. Puustinen, J. Lappalainen, P. Karioja, and R. Myllyla, "Fabrication of optical inverted-rib waveguides using UV-imprinting," Microelectron. Eng. **88**(2), 175–178 (2011).
19. X. Lin, X. Dou, X. Wang, and R. T. Chen, "Nickel electroplating for nanostructure mold fabrication," J. Nanosci. Nanotechnol. **11**(8), 7006–7010 (2011).
20. X. Y. Dou, X. L. Wang, H. Y. Huang, X. H. Lin, and R. T. Chen, "Fabrication of metallic hard mold for polymeric waveguides with embedded micro-mirrors," 2010 IEEE Photonics Society Winter Topicals Meeting Series, 101–102 (2010).
21. T. Ling, S. L. Chen, and L. J. Guo, "Fabrication and characterization of high Q polymer micro-ring resonator and its application as a sensitive ultrasonic detector," Opt. Express **19**(2), 861–869 (2011).
22. D. Pisignano, L. Persano, E. Mele, P. Visconti, M. Anni, G. Gigli, R. Cingolani, L. Favaretto, and G. Barbarella, "First-order imprinted organic distributed feedback lasers," Synth. Met. **153**(1-3), 237–240 (2005).
23. P. C. Kao, S. Y. Chu, T. Y. Chen, C. Y. Zhan, F. C. Hong, C. Y. Chang, L. C. Hsu, W. C. Liao, and M. H. Hon, "Fabrication of large-scaled organic light emitting devices on the flexible substrates using low-pressure imprinting lithography," IEEE Trans. Electron. Dev. **52**(8), 1722–1726 (2005).
24. Y. Ekinci, H. H. Solak, C. David, and H. Sigg, "Bilayer Al wire-grids as broadband and high-performance polarizers," Opt. Express **14**(6), 2323–2334 (2006).
25. B. Ciftcioglu, R. Berman, S. Wang, J. Y. Hu, I. Savidis, M. Jain, D. Moore, M. Huang, E. G. Friedman, G. Wicks, and H. Wu, "3-D integrated heterogeneous intra-chip free-space optical interconnect," Opt. Express **20**(4), 4331–4345 (2012).
26. C. H. Tien, C. H. Hung, and T. H. Yu, "Microlens arrays by direct-writing inkjet print for lcd backlighting applications," J Disp Technol **5**(5), 147–151 (2009).
27. S. R. Mohapatra, T. Tsuruoka, T. Hasegawa, K. Terabe, and M. Aono, "Flexible resistive switching memory using inkjet printing of a solid polymer electrolyte," AIP Adv. **2** (2012).
28. Y.-T. Han, J.-U. Shin, S.-H. Park, H.-J. Lee, W.-Y. Hwang, H.-H. Park, and Y. Baek, "N × N polymer matrix switches using thermo-optic total-internal-reflection switch," Opt. Express **20**(12), 13284–13295 (2012).
29. Y. O. Noh, H. J. Lee, Y. H. Won, and M. C. Oh, "Polymer waveguide thermo-optic switches with - 70 dB optical crosstalk," Opt. Commun. **258**(1), 18–22 (2006).
30. X. L. Wang, B. Howley, M. Y. Chen, Q. J. Zhou, R. Chen, and P. Basile, "Polymer based thermo-optic switch for optical true time delay," Integrated Optics: Devices, Materials, and Technologies IX **5728**, 60–67 (2005).
31. M. G. Kang and L. J. Guo, "Metal transfer assisted nanolithography on rigid and flexible substrates," J. Vac. Sci. Technol. B **26**(6), 2421–2425 (2008).

1. Introduction

Polymer photonics is an important branch in modern integrated optics. It is compatible with Si and GaAs fabrication technologies [1], and provides a good platform for integrating various active and passive devices, including polymer DBF lasers [2], optical bus waveguides [3], optical switches [4, 5], optical modulators [6–8], etc. The most common method for polymer optical device fabrication includes using high energy reactive ion-beam (RIE) to define the pattern into a resist, and further transfer the pattern to the optical polymer via plasma etching. This method is straightforward, but not a cost-effective way due to complicated fabrication process and low throughput. Another method is to directly pattern a low loss UV-curable polymer using lithography [9]. However, this method is limited due to poor dimension and profile control resulting from the effects of wave diffraction, interface and substrate scattering [10]. Molding/imprinting method can effectively overcome these shortcomings, and can potentially provide roll-to-roll (R2R) patterning capabilities at both micro- and nano-scales, thus providing a viable solution for the high-rate development of low cost polymer photonic devices [11]. Although extensive research has been conducted on using various kinds of molds to pattern basic optical components such as micro-lens array [12, 13], polymer gratings [11, 14, 15], optical waveguides with different dimensions [16–20], micro-ring resonators [21]etc., work demonstrating complete functional devices using imprinting method have been limited [10, 22–24]. Another less explored method for fabricating polymer photonic devices is ink-jet printing. Ink-jet is a digital printing method which has a good potential for complementing imprinting method for the development of photonic devices. Using ink-jet printing alone, several applications have been reported, including micro-lenses [25, 26] and polymer electrolyte for memory cells [27]. With this drop-on-demand technique, precise material placement is achievable with minimal material wastage. Additionally, due to its non-contact form of printing, it possesses least risk for

#179234 - $15.00 USD Received 8 Nov 2012; accepted 26 Dec 2012; published 18 Jan 2013

integration with imprinting since the potential damage for the imprinted delicate structures is minimal.

In this paper, utilizing the precise structural patterning capabilities of imprinting method, and integrating precise material placement advantages offered by ink-jet printing technique in the process flow, we successfully fabricate a 2 × 2 thermo-optic (TO) switch, and experimentally demonstrate its operation up to 1 kHz. To our knowledge, this is the first demonstration of a printable photonic device. The potential R2R imprinting method, together with ink-jet printing process, could provide great potential solution for the development of flexible and low cost integrated photonic devices with high yield.

2. Device design

2.1 Material system

In order to enable device development, the material system choice should meet certain criteria: First, all the materials should satisfy the optical index requirement to form a waveguide. Second, the bottom cladding layer should be imprintable. Third, the core layer should have sufficient thermo-optic coefficient so that a suitable change in the index is achieved within a small temperature gradient. Fourth, the core material should have suitable viscosity to be ink-jet printed. In order to satisfy the physical and optical characteristics, we selected UV15LV (n = 1.501@1.55μm) from MasterBond as the bottom cladding layer, SU8-2000.5 (n = 1.575@1.55μm) from MicroChem as the core layer and UFC-170A (n = 1.496@1.55μm) from URAY Co. Ltd as top cladding layer. Of the three layers, the bottom cladding material UV15LV and the core layer material SU-8 2000.5 are ink-jet printable. Although LFR/ZPU series TO polymer from ChemOptics, Korea, with its high TO coefficient of ~-2.5 x 10^{-4}/K @1.55μm, is an ideal choice for TO polymer switch development [5, 28, 29], its relatively lower refractive index (n < 1.48) compared to UV15LV, rules out its use as a core material. Moreover, the wide availability, low cost, great stability and higher refractive index of SU-8 polymer are beneficial for low cost polymer device development in spite of its lower TO coefficient of −1.1 x 10^{-4}/K @1.55μm.

2.2 Optical and thermal design of the 2 × 2 thermo-optic polymer TIR switch

A schematic of the 2 × 2 thermo-optic polymer TIR switch is shown in Fig. 1(a). The design of the switch includes two major parts: the optical design and the thermal design. The optical path and waveguide cross section are designed and simulated, as shown in Figs. 1(a)-1(c), with a horn structure. A rib waveguide structure is used and the core layer consists of a 1.8 μm thick slab and a 5 μm (width) × 0.5 μm (thick) strip. The separation of two input and two output waveguides is set at 250 μm, which is compatible with a standard fiber array. A curved waveguide with 10mm bending radius is used to guide light from the input port to the X junction. A horn structure [30] is used at the junction, with a maximum width of 40 μm at the center. The half branch angle for the X junction is optimized at 4° based on the consideration of cross-talk minimization and switching power trade-off. Larger junction angle requires more power to switch the light while smaller junction angle will increase the cross-talk between two ports. Besides, the horn structure is also compatible with the temperature gradient generated by the heating element. The heating element is designed to have a width of 8 μm at the center. Due to its thinness compared to other connecting parts, most of heat is generated at the center region only. Due to the relatively thin electrode, when heated up, the temperature difference between the electrode and the SU-8 layer is less than 5°C, according to simulation. If it is assumed that only the polymer layers beneath the heating electrode undergo a change in refractive index, a −0.02 index change in the SU-8 layer is needed for reflecting all of the input light from one arm to the other at the X junction. Since SU-8 has a thermo-optic coefficient of -1.1×10^{-4}/K, the temperature change required is over 180°C. However, in reality, the heat distribution beneath the electrode takes a Gaussian profile. Therefore, the adjacent polymer will also get heated up, thus lower the temperature change required, and thus, the electrical power needed to total internally reflect the light. The

#179234 - $15.00 USD Received 8 Nov 2012; accepted 26 Dec 2012; published 18 Jan 2013

simulated fundamental mode in the waveguide are shown in Fig. 1(b), where the mode is well confined within the waveguide region and does not extend more than 3μm into the cladding, which helps in reducing the absorption loss from the gold heating electrode. The simulated powers in the bar (blue) and the cross (green) ports for the switching condition are also shown in Fig. 1(c).

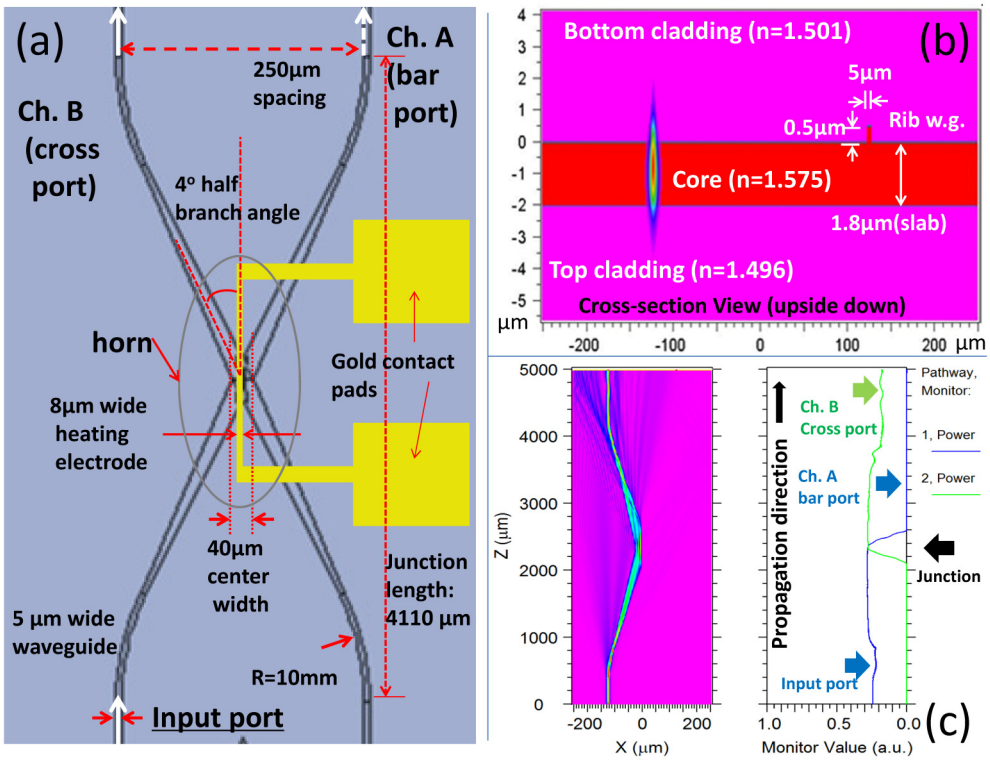

Fig. 1. (a) schematic showing the top view of the 2 × 2 thermo-optic switch layout. A horn structure, with a half branch angle of 4° is used. Gold heating electrode is 8 μm wide over the center region of the horn. (b) The cross-section view and the simulated mode profile at the input side of the 2 × 2 TO switch. The mode is well confined in the waveguide. Core layer is composed of 1.8 μm thick slab and 0.5 μm (height) x 5 μm (width) strip. (c) Simulation results of the power outputs from the bar (blue) and the cross (green) ports when the junction is in switching condition

3. Fabrication process

Traditionally, thermo-optic polymer TIR switches utilizing channel waveguide or rib waveguide structures are fabricated utilizing reactive ion etching method. The high energy bombardment in the reactive ion etching process is capable of removing polymer materials using photo-resist or metal as an etching mask. The disadvantages of this method include long fabrication time, low throughput and high cost. In the present research, a UV based imprinting method is employed to define the waveguide channel. Also, this method is compatible with roll-to-roll processing, and has the potential for high speed, low cost device fabrication. For the presented thermo-optic switch, besides imprinting, we also integrate an ink-jet printing method to deposit the core layer. The fabrication process flow is shown in Fig. 2. First, a flexible mold is fabricated using a silicon hard mold. The flexible mold is then used to define the core region in a UV15LV bottom cladding layer, which is coated on a silicon substrate [Fig. 2(b)]. Following this step, an ink-jet printer is used to print a layer of SU8 2000.5, which not only fills the core trench, but also forms a planar top surface for further processing [Fig. 2 (c)]. Upon curing, another layer of UV15LV is ink-jet printed on

#179234 - $15.00 USD
Received 8 Nov 2012; accepted 26 Dec 2012; published 18 Jan 2013

top to form the top cladding layer. Please note that we have found the gold heater electrode fabrication process (lift-off method) incompatible with the printed UV15LV layer. Therefore, for demonstrations, we have chosen UFC-170A as a top cladding layer. In future, by switching to another R2R process for electrode transfer [31], UV15LV can replace UFC-170A. The detailed fabrication steps are provided in the following sub-sections.

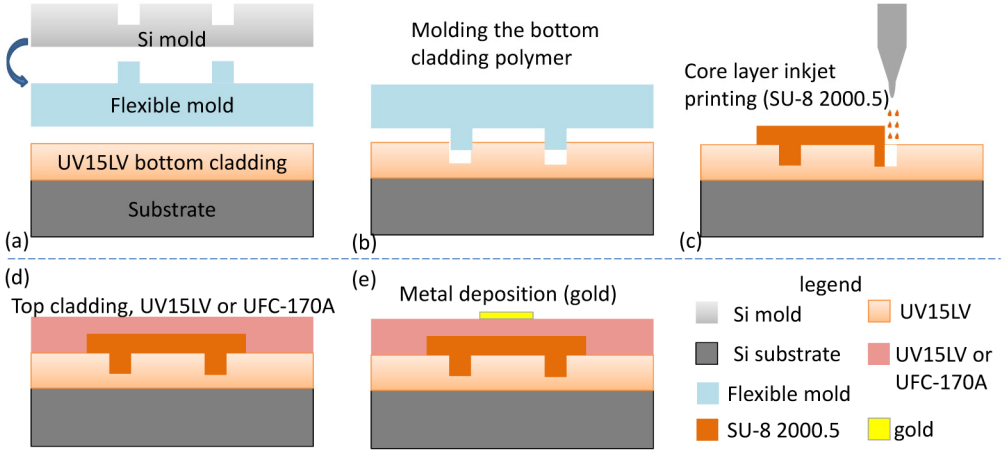

Fig. 2. Process flow for fabricating a 2 × 2 thermo-optic polymer switch using imprinting and ink-jet printing method

3.1 Mold fabrication

Imprint mold fabrication is a critical step for determining device performance. The hard and soft mold fabrication processes are shown in Figs. 3(a) and 3(b), respectively. We start with a 4" silicon wafer for master mold fabrication. A 50nm layer of silicon dioxide is deposited onto the silicon wafer using PECVD. A 900 nm thick photoresist is then spin coated on top and patterned to form an etching mask for the oxide layer. The waveguide pattern on the photoresist is then transferred to the oxide layer via dry etching using RIE. Then, silicon is etched by RIE using silicon dioxide as hard mask. Due to the high selectivity of silicon oxide and silicon, vertical sidewall is achieved. The etching depth is chosen to be 0.5 μm. After silicon etching, the oxide hard mask is removed by buffered oxide etch (BOE), which completes the master mold fabrication. Then, the fabricated silicon master mold is used to fabricate a transparent flexible mold on a polyethylene terephthalate (PET) substrate. The transparent flexible mold fabrication starts from spin-coating a photo-curable silsesquioxane (SSQ) resist on the PET substrate at 2000 rpm for 60s, which results in a thickness of around 2 μm for the film. After that, the sample is pre-baked on a hot-plate at 100°C for 5 minutes to remove the solvent. At the same time, the master silicon mold is cleaned in piranha solution for 30mins to grow a thin layer of fresh silicon oxide layer. Then, the master mold is vapor-coated with an anti-sticking layer. After the anti-sticking layer coating, the SSQ coated PET substrate is placed on the top of the silicon master mold. Then, the sample is placed inside a pressure chamber to perform a UV imprinting process at 250 psi. After the SSQ resist is fully cured, the master mold and the PET substrate are separated by de-molding process. Thus, the SSQ mold is successfully fabricated on the transparent flexible PET substrate. The advantage of using two types of molds is that, even if the soft mold degrades after several imprinting processes, it can readily be duplicated from the original silicon master mold.

#179234 - $15.00 USD
Received 8 Nov 2012; accepted 26 Dec 2012; published 18 Jan 2013

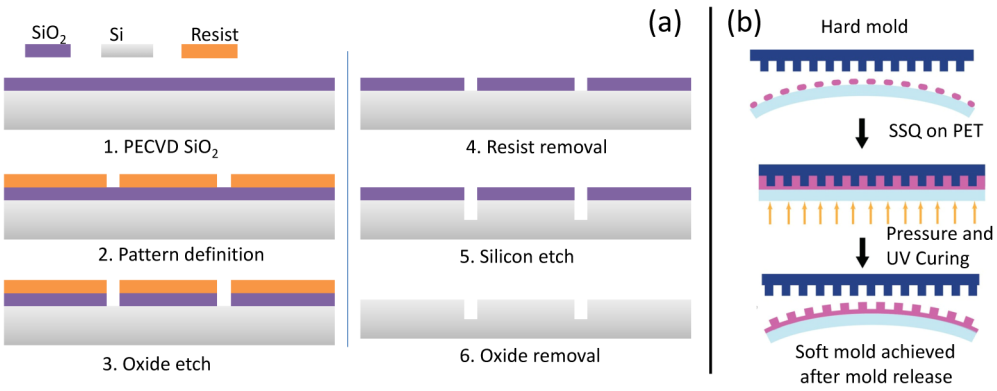

Fig. 3. (a) silicon master mold fabrication process (b) soft mold replication from master mold

3.2 UV-imprinting

The UV imprinting process is used for transferring the pattern from the soft mold to the bottom cladding polymer (UV15LV). First, the fabricated transparent flexible SSQ mold is vapor-coated with anti-sticking layer at 100°C for 1 hour. Then, the SSQ mold is brought into conformal contact with a silicon wafer coated with UV15LV resist. After that, a UV-imprinting process is performed in a pressure chamber with a pressure at 250 psi. Then, the imprinted UV15LV resist is fully cured by exposure to UV light for more than 5mins. The SEM images at the junction area of the silicon master mold, SSQ soft mold and the molded trench on UV15LV are shown in Figs. 4(a), 4(b) and 4(c), respectively.

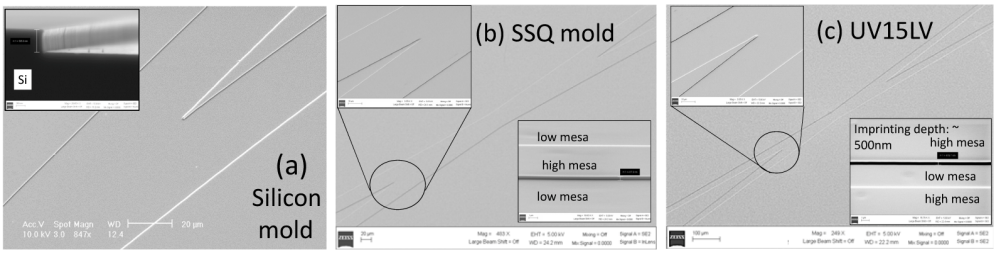

Fig. 4. SEM images of (a) silicon mold (b) SSQ soft mold (c) imprinted UV 15LV at the junction area of the TO switch. The inset in (a) shows the cross-section views of the silicon mold, with 500nm step height. The upper left insets in (b) and (c) show the zoom-in views of the merging points of two waveguides. The lower right insets in (b) and (c) shows the tilted view of mold and imprinted trench in the 5 μm wide input/output regions

3.3 Ink-jet printing

The printer employed in this research is a Fujifilm Dimatix Materials Printer (DMP-2800). It utilizes a piezoelectric cartridge to jet material onto a desired area on the substrate. The material choice is wide as long as its viscosity is between 10 and 12 cPs ($1.0x10^{-2}$ - $1.2x10^{-2}$ Pa·s), and surface tension is between 28 and 33 dynes/cm (0.028 - 0.033 N/m) at operating temperature. With the aid of a fiducial camera, the printing region can be defined within a positional error of 25 μm. This type of a non-contact printing method is topography independent, thus, it can fill the trench in the imprinted UV15LV layer while still keeping a flat top. Additionally, it can easily be extended to a roll-to-roll process.

As mentioned above, SU-8 2000.5 resist is used as the core layer. The jetting profile in the printer is optimized to ensure a uniform printed layer. The parameters can be controlled to tune the layer thickness between 1 and 2 μm. The printed SU-8 also fills the patterned waveguide region in the UV15LV bottom cladding layer to form a rib waveguide structure.

#179234 - $15.00 USD
Received 8 Nov 2012; accepted 26 Dec 2012; published 18 Jan 2013

After printing, the substrate is pre-baked at 90°C to remove the solvent and then exposed to UV for 30s, followed by post-baking to fully cross-link the SU-8 layer. Following this step, another layer of UV15LV is ink-jet printed on top and cured to form the top cladding layer. SEM cross section image of the fully printed device is shown in Fig. 5(a). However, as mentioned above, due to incompatibility of UV15LV with the following electrode formation process, a 3 μm thick UFC-170A polymer is used as the top cladding layer for device demonstration, as shown in Fig. 5(b). We will use a roll-to-roll compatible electrode transfer method [31] in future to overcome this problem.

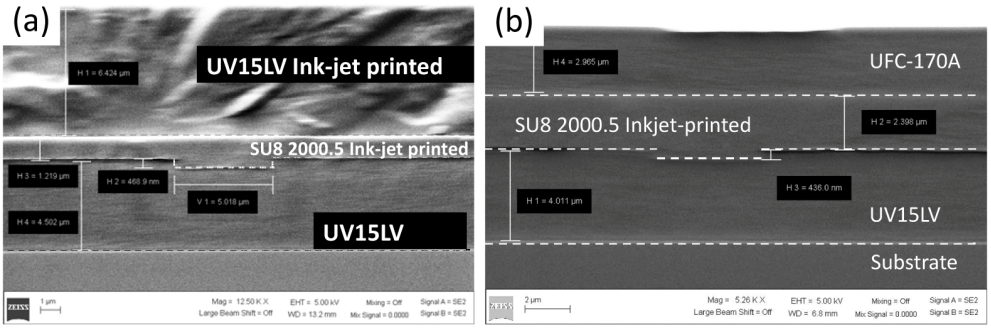

Fig. 5. SEM cross-section view of printed layers in the device, (a) with ink-jet printed UV15LV as top cladding (b) with coated UFC-170A as top cladding

Compared to spin-coating method, comparable film quality can be achieved using ink-jet printing, with an added advantage that the printing method is more flexible because one can easily define the region of material placement, without going through an additional photolithography step. It will also reduce the potential risk of material incompatibility issue that may occur during photolithography.

3.4 Electrode deposition

After curing the top cladding layer, standard image reversal and lift-off processes are performed to deposit a gold heating electrode on the top. The heating element covering the junction area at the center is 8 μm wide and 500 μm long. An optical microscopic image of the fabricated device is shown in Fig. 6(a).

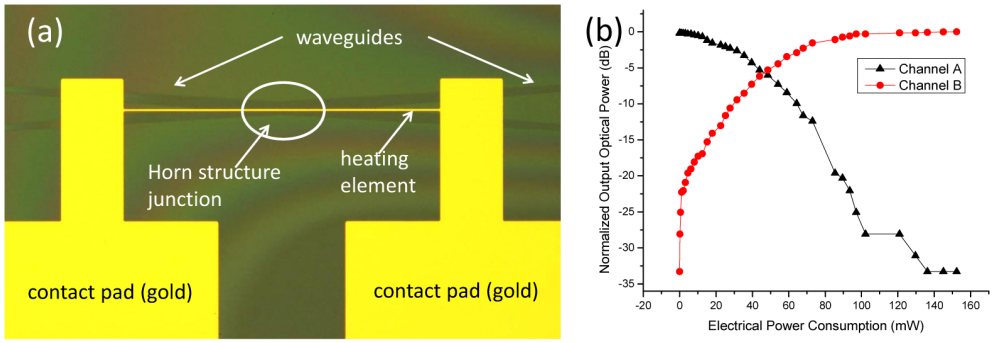

Fig. 6. (a) Microscopic picture showing the top view of a fabricated 2 × 2 thermo-optic polymer switch. (b) Normalized optical output power versus electrical power consumption from both bar port (Channel A) and cross port (Channel B).

4. Device testing

The testing is performed with the aid of auto aligner system. The input light at a wavelength of 1550nm wavelength is launched into one port of the device using a lensed fiber. A DC

#179234 - $15.00 USD Received 8 Nov 2012; accepted 26 Dec 2012; published 18 Jan 2013

voltage from a power supply is applied across the heating elements using probes. An ammeter is used to monitor the real-time current, which is required in order to calculate the overall power consumption. To examine the performance of switching behavior at different applied voltages, output light power from two output channels of the device, as well as the current reading on the ammeter are recorded. Figure 6(b) shows the normalized optical output power versus the electrical power consumption. It takes around 100mW power for the cross port to reach its maximum output.

Response speed is another important parameter for a switch. A function generator is used to generate a square wave signal at different frequencies and applied across the heating electrode. The optical response at each frequency is measured using an oscilloscope is shown in Fig. 7. It can clearly be seen from the figure that device operates up to a frequency of 1 kHz. We also measured the rising/falling time of the device to be 0.46ms/0.40ms. The rising time for bar port and falling time for cross port are relatively longer because they correspond to the OFF state of the applied signal, wherein the junction needs more time to dissipate the heat, compared to the time needed to heat up the polymer.

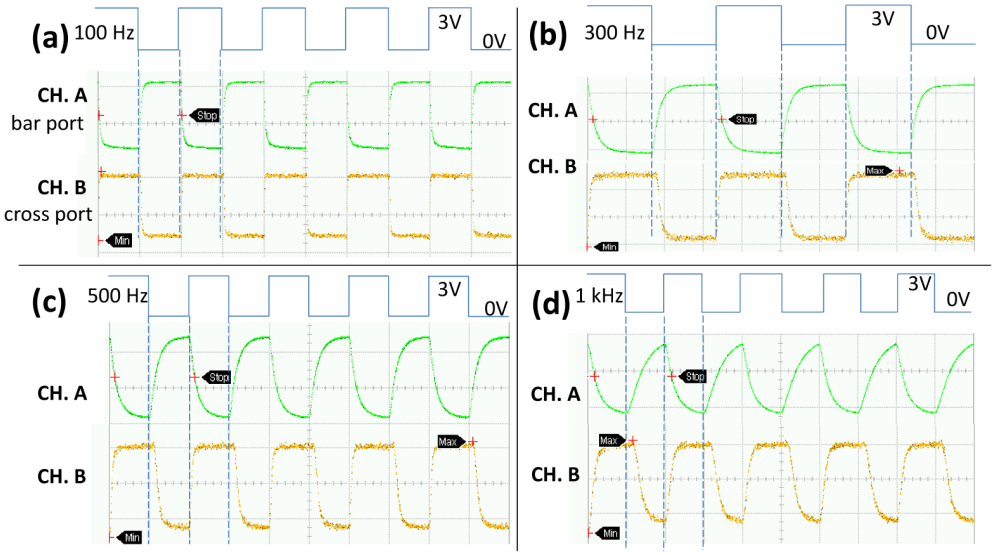

Fig. 7. Optical response with square wave function applied across the heating electrode, at selected frequencies of (a) 100Hz, (b) 300Hz, (c) 500Hz, and (d) 1kHz. The device can operate at 1kHz with decent performance. Channel A represents bar port and Channel B represents cross port.

5. Conclusion

In this paper, we demonstrated a fully functional thermo-optic polymer 2 × 2 switch utilizing imprinting and ink-jet printing methods. Compared to traditional method, the printable method provides greater feasibility in the fabrication process. Operation of the switch is experimentally demonstrated up to a frequency of 1 kHz, with less than 0.5ms switching time. The fabrication processes involved are fully roll-to-roll compatible, which can enable high throughput, low cost and volume manufacturing of photonic devices.

Acknowledgments

This work was supported by the Air Force Office of Scientific Research (AFOSR) STTR contract FA9550-12-C-0052 monitored by Dr. Gernot Pomrenke. The fabrication and characterization were performed at the Microelectronics Research Center (MRC) of The University of Texas at Austin and Lurie nanofabrication facility in University of Michigan, Ann Arbor.

#179234 - $15.00 USD Received 8 Nov 2012; accepted 26 Dec 2012; published 18 Jan 2013